Received: 6 November 2023 | Revised: 27 March 2024 | Accepted: 6 April 2024

DOI: 10.1111/cas.16190

ORIGINAL ARTICLE

Cancer Science WILEY

Long noncoding RNA SNHG3 interacts with microRNA-502-3p to mediate ITGA6 expression in liver hepatocellular carcinoma

Juncheng Guo[1] | Jianquan Zhang[2] | Yang Xiang[2] | Shuai Zhou[2] | Yijun Yang[2] | Jinfang Zheng[3]

[1]Postdoctoral Workstation, Central South University Xiangya School of Medicine Affiliated Haikou Hospital, Haikou, Hainan, China

[2]Department of Surgery, Central South University Xiangya School of Medicine Affiliated Haikou Hospital, Haikou, Hainan, China

[3]Department of Hepatobiliary Surgery, Hainan Provincial People's Hospital, Haikou, Hainan, China

Correspondence
Yijun Yang, Department of Surgery, Central South University Xiangya School of Medicine Affiliated Haikou Hospital, No. 43, Renmin Avenue, Haikou 570208, Hainan, China.
Email: yangyijun168@163.com

Jinfang Zheng, Department of Hepatobiliary Surgery, Hainan Provincial People's Hospital, Haikou 570311, Hainan, China.
Email: zhengjf2000@hainmc.edu.cn

Funding information
Science and Technology Project of Hainan Province, Grant/Award Number: ZDYF2022SHFZ117

Abstract

SNHG3, a long noncoding RNA (lncRNA), has been linked to poor outcomes in patients with liver hepatocellular carcinoma (LIHC). In this study, we found that SNHG3 was overexpressed in LIHC and associated with poor outcomes in patients with LIHC. Functional assays, including colony formation, spheroid formation, and in vivo assays showed that SNHG3 promoted stemness of cancer stem cells (CSC) and tumor growth in vivo by interacting with microRNA-502-3p (miR-502-3p). miR-502-3p inhibitor repressed the tumor-suppressing effects of SNHG3 depletion. Finally, by RNA pull-down, dual-luciferase reporter assay, m6A methylation level detection, and m6A-IP-qPCR assays, we found that miR-502-3p targeted YTHDF3 to regulate the translation of integrin alpha-6 (ITGA6) and targeted HBXIP to inhibit the m6A modification of ITGA6 through methyltransferase-like 3 (METTL3). Our study revealed that SNHG3 controls the YTHDF3/ITGA6 and HBXIP/METTL3/ITGA6 pathways by repressing miR-502-3p expression to sustain the self-renewal properties of CSC in LIHC.

KEYWORDS
cancer stem cells, ITGA6, liver hepatocellular carcinoma, long noncoding RNA SNHG3, microRNA-502-3p

1 | INTRODUCTION

With a 5-year survival of 18%, liver cancer is the second most lethal tumor after pancreatic cancer.[1] For patients with early-stage liver hepatocellular carcinoma (LIHC) with no history of cirrhosis or portal hypertension, resection is recommended, but it is associated with a recurrence rate of approximately 60%–70% at 5 years.[2] The majority of patients with the most frequent subtype of LIHC are diagnosed at advanced stages, at which treatment options are limited to systemic therapy.[3] Cancer stem cells (CSC), a small population of tumor

Abbreviations: CSC, cancer stem cells; DMEM, Dulbecco's modified Eagle's medium; FBS, fetal bovine serum; FISH, fluorescence in situ hybridization; HBXIP, hepatitis B virus X-interacting protein; ITGA6, integrin alpha-6; LIHC, liver hepatocellular carcinoma; METTL3, methyltransferase-like 3; RIP, RNA immunoprecipitation; SNHG3, small nucleolar RNA host gene 3; YTHDF3, YTH domain-containing family protein 3.

Juncheng Guo and Jianquan Zhang contributed equally to this work.

This is an open access article under the terms of the Creative Commons Attribution-NonCommercial-NoDerivs License, which permits use and distribution in any medium, provided the original work is properly cited, the use is non-commercial and no modifications or adaptations are made.
© 2024 The Authors. *Cancer Science* published by John Wiley & Sons Australia, Ltd on behalf of Japanese Cancer Association.

cells, have been revealed to hold highly tumorigenic, metastatic, and chemotherapy- and radiation-resistant properties, thus resulting in relapse after therapy.[4] Therefore, studying the molecular crosstalk underlying the maintenance of CSC in LIHC is of great value in improving patient prognosis.

The significance of long noncoding RNAs (lncRNAs) in the initiation and progression of LIHC has been appreciated because they govern the proliferation, apoptosis, vessel formation, and invasive ability of cancer cells by binding to DNA, RNA, or proteins.[5] Mechanistically, the competing endogenous RNA (ceRNA) model describes lncRNAs as sponges for microRNAs (miRNAs) to indirectly modulate the targets of miRNAs.[6] SNHGs are a family of lncRNAs that are overexpressed in many malignancies, including respiratory and digestive tumors.[7] SNHG3 primarily competes as a ceRNA that targets tumor suppressor miRNAs, thereby regulating biological processes in tumors.[8] Moreover, SNHG3 has been identified as one of the 11 CSC-related lncRNAs with prognostic value in LIHC.[9] However, its functional role in regulating CSC in LIHC remains unclear. By intersection of differentially expressed miRNAs in the GSE108724 and GSE166348 datasets and possible targets of SNHG3 in the Starbase website (https://starbase.sysu.edu.cn/index.php), we obtained four candidates: hsa-miR-500a-3p, hsa-miR-502-3p, hsa-miR-151a-3p, and hsa-miR-196b-5p. Only miR-502-3p has not been reported to be related to the stemness of CSC.[10–12] Therefore, we selected miR-502-3p for subsequent assays.

We previously reported that miR-448 targets YTHDF3, thus controlling the expression of ITGA6,[13] a factor generally used to identify CSC populations and sustain the self-renewal of CSC.[14] In contrast, HBXIP was shown to potentiate the malignant biological behaviors of LIHC cells via N6-methyladenosine (m6A) modification of hypoxia-inducible factor-1α in a METTL3-dependent manner.[15] Intriguingly, METTL3 catalyzes the m6A modification of ITGA6, thereby encouraging the translation of ITGA6 mRNA.[16] These data led us to hypothesize that HBXIP and YTHDF3 are the putative targets of miR-502-3p. The motivation and innovation of this study was to decode the interaction between SNHG3 and miR-502-3p in two possible pathways, the YTHDF3/ITGA6 axis and the HBXIP/METTL3/ITGA6 axis in LIHC, thereby providing an understanding of the role of SNHG3 in LIHC.

2 | MATERIALS AND METHODS

2.1 | Tumor tissue collection

Cancerous and adjacent tissues resected from 86 patients who had been diagnosed with LIHC at the Central South University Xiangya School of Medicine Affiliated Haikou Hospital between March 2019 and March 2021 were collected. None of the patients had received chemotherapy or drugs before surgery. The patients were followed up every 2 months after surgery, with a total follow-up period of 12 months. The study was approved by the Ethics Committee of Central South University Xiangya School of Medicine Affiliated Haikou Hospital, in compliance with the Declaration of Helsinki. Informed consent was obtained from all patients.

2.2 | Cell culture and lentiviral infection

Huh7 and PLC/PRF/5 cells were cultured in DMEM/F12 containing 10% FBS, 100 μg/mL penicillin, and 100 U/mL streptomycin. For CSC isolation, Huh7 and PLC/PRF/5 cells were grown in serum-free DMEM/F12 medium (Thermo Fisher Scientific Inc.) with penicillin–streptomycin, B27 supplement, 20 ng/mL EGF, 20 ng/mL bFGF, and N2 supplement for 2 weeks. The medium was renewed every 3 days. The cells forming spheres in the supernatant were made into single-cell suspensions (termed PLC/PRF/5/CSC or Huh7/CSC). The CSC markers, CD13 and CD133, were subsequently identified using flow cytometry. PLC/PRF/5/CSC or Huh7/CSC cells were cultured in DMEM/F12 plus penicillin–streptomycin, B27 supplement, 20 ng/mL EGF, 20 ng/mL bFGF, and N2 supplement at 37°C with 5% CO_2.

The lentiviral vectors were designed and constructed by GenePharma. Huh7/CSC and PLC/PRF/5/CSC cells were infected with different lentiviral vectors for 72 h. Positive cells were screened using puromycin, and the effect of infection was verified by RT-qPCR or Western blot. Detailed methods of malignant phenotype measurements and binding relation assessments can be found in Appendix S1.

2.3 | RT-qPCR

The TRIzol kit was used for total RNA extraction, and a PrimeScript™ RT reagent kit (RR037Q, Takara Biotechnology Ltd.) was used for reverse transcription. TB Green® Premix Ex Taq™ II (RR820Q; Takara) was used for qPCR. Quantitative analysis of miRNA was performed using the Mir-X miRNA qRT-PCR TB Green Kit (638314, Takara). mRNA or miRNA expression was normalized to β-actin or U6 and calculated using the $2^{-\Delta\Delta Ct}$ method. Primers used are listed in Table 1.

2.4 | Western blot

Cells or tissues were lysed in RIPA lysis buffer containing 1% protease inhibitor with 1% phosphatase inhibitor. The proteins were separated by SDS-PAGE and transferred to PVDF membranes. The membranes were sequentially sealed with goat serum and incubated with primary antibodies (Appendix S1) overnight at 4°C and with HRP-conjugated goat anti-rabbit secondary antibody (1:2000, ab6721, Abcam) for 120 min at room temperature. An ECL kit was used for protein development, and band intensity was analyzed using ImageJ software.

TABLE 1 Primer sequences.

Gene	Forward sequence (5′-3′)	Reverse sequence (5′-3′)
SNHG3	GACTTCCGGGCACTTCGTAA	TGCTCCAAGTCTGCCAAAGA
miR-502-3p	TCCTTGCTATCTGGGTG	GAACATGTCTGCGTATCTC
YTHDF3	GCTACTTTCAAGCATACCACCTC	ACAGGACATCTTCATACGGTTATTG
HBXIP	TGTTCTAGCCCAGCAAGCAGCT	CGTGATGCCATCGTGTTTCTGG
ITGA6	CGAAACCAAGGTTCTGAGCCCA	CTTGGATCTCCACTGAGGCAGT
METTL3	CTATCTCCTGGCACTCGCAAGA	GCTTGAACCGTGCAACCACATC
β-actin	CACCATTGGCAATGAGCGGTTC	AGGTCTTTGCGGATGTCCACGT
U6	CTCGCTTCGGCAGCACAT	TTTGCGTGTCATCCTTGCG

Abbreviations: HBXIP, hepatitis B virus X-interacting protein; ITGA6, integrin alpha-6; METTL3, methyltransferase-like 3; miR-502-3p, microRNA-502-3p; SNHG3, small nucleolar RNA host gene 3; YTHDF3, YTH domain-containing family protein 3.

2.5 | Animal studies

The experimental protocol was authorized by the ethics committee of the Central South University Xiangya School of Medicine Affiliated Haikou Hospital and conformed to the Guide for the Care and Use of Laboratory Animals. Five-week-old male BALB/c nude mice ($n=120$, Vital River) were maintained under specific pathogen-free (SPF) conditions.

For tumor growth assessment, 10^4 Huh7/CSC infected with different lentiviral vectors were mixed with Matrigel at a 1:1 ratio, and the mixture was injected subcutaneously into nude mice ($n=6$). Tumor volume was assessed every other week during the experiment using the following formula: (long diameter × short diameter^2)/2. At week 5 after injection, the nude mice were euthanized using 150 mg/kg sodium pentobarbital. The tumor tissues were weighed, and 4-μm paraffin sections were prepared from the tumor tissues after embedding in paraffin.

For mouse survival assessment, a mixture of 10^5 infected Huh7/CSC cells with Matrigel was administered to the liver of nude mice. The mice were monitored daily, and the time of death was recorded. The mortality rate of the mice was analyzed after the death of the last mouse in each group ($n=6$).

2.6 | Immunohistochemistry

Paraffin-embedded sections of subcutaneous tumor tissues were dewaxed, rehydrated, and heated for antigen retrieval. Goat serum sealing was performed to avoid nonspecific binding. The sections were probed with the antibody against KI67 (1:200, ab15580, Abcam) overnight at 4°C and with goat anti-rabbit secondary antibody (1:1000, ab6721, Abcam) for 0.5 h at room temperature. The sections were stained with DAB, and positivity was observed under a light microscope.

2.7 | Statistical analyses

All data were analyzed using GraphPad Prism 8.0 (GraphPad) and are indicated as mean ± SD. Comparisons between the two groups were analyzed using paired or unpaired *t*-tests. The data among multiple groups were analyzed using one-way or two-way ANOVA and Tukey's post-hoc test. Kaplan–Meier analysis was used to generate survival curves, and Pearson's correlation coefficient was used to evaluate the correlation of indicators. Statistical significance was set at $p<0.05$.

3 | RESULTS AND DISCUSSION

The oncogenic role of SNHG3 has been indicated in bladder cancer,[17] non-small cell lung cancer,[18] oral squamous cell carcinoma,[19] and gastric cancer.[20] More importantly, SNHG3 has been reported to induce epithelial–mesenchymal transition and sorafenib resistance by mediating the miR-128/CD151 pathway in LIHC.[21] However, there are no clues regarding the sustained effects of SNHG3 on CSC in LIHC.

3.1 | SNHG3 is overexpressed in LIHC and linked to the stemness of LIHC cells

In the UALCAN database (http://ualcan.path.uab.edu/index.html), SNHG3 was found to be overexpressed in LIHC (Figure 1A), which was associated with poor patient prognosis (Figure 1B). RT-qPCR and FISH in tumors and adjacent tissues from our cohort showed overexpression of SNHG3 in tumor tissues (Figure S1A,B). Patients were categorized into high- and low-SNHG3-expression groups based on median SNHG3 expression. Survival was worse in patients with high SNHG3 expression levels (Figure S1C). CSCs are regulated by the expression of several stemness-associated genes, such as SOX2 and Nanog, and CSCs within LIHC are mostly marked by various surface markers, including EpCAM.[22] Intriguingly, the expression of SNHG3 was positively correlated with EpCAM, Nanog, and SOX2 expression (Figure S1D).

We isolated Huh7/CSC and PLC/PRF/5/CSC, and flow cytometry analysis of the CSC markers CD13 and CD133 confirmed the successful isolation of Huh7/CSC and PLC/PRF/5/CSC (Figure 1C). A much higher expression of stemness-related genes was observed

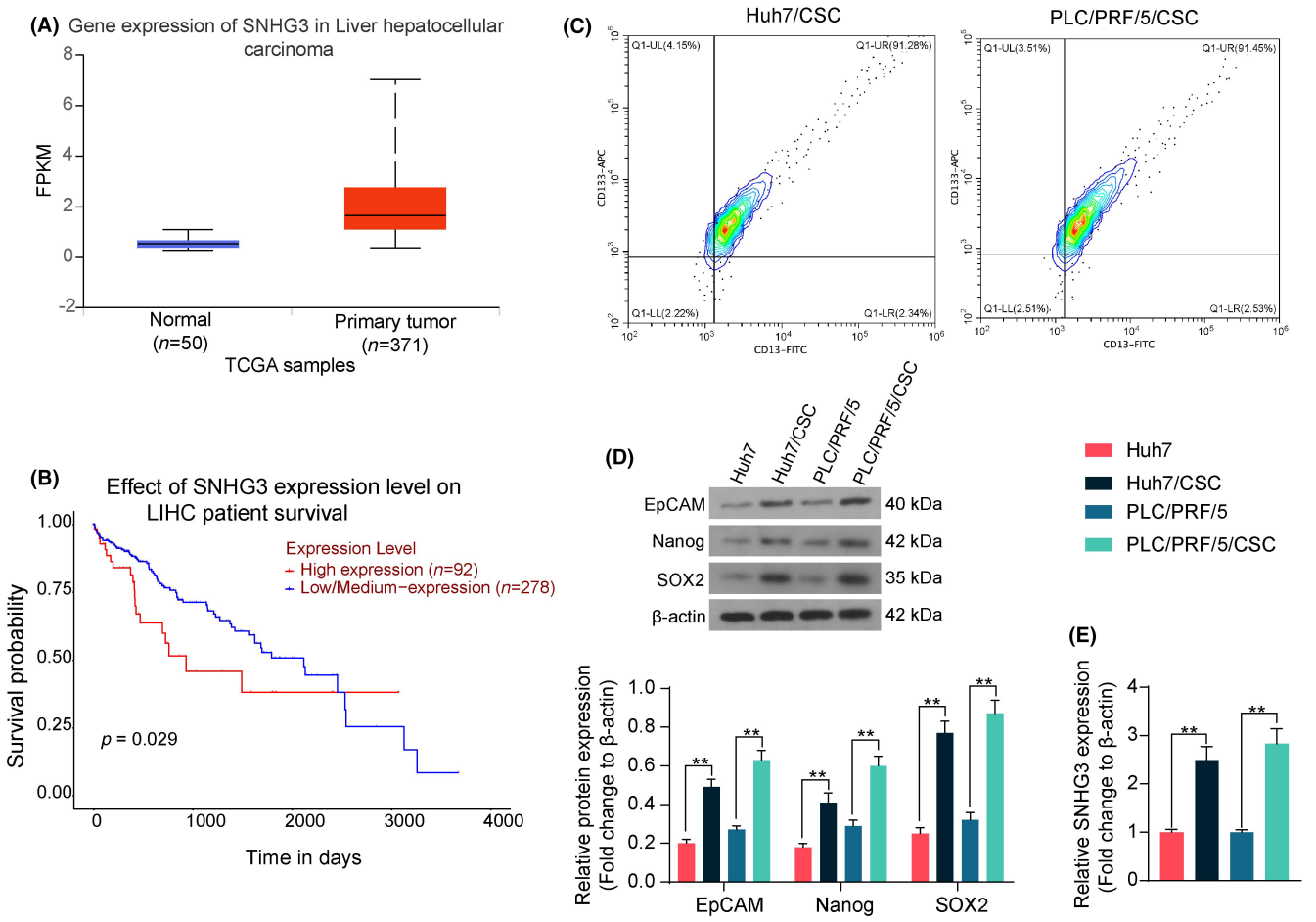

FIGURE 1 Overexpression of SNHG3 in liver hepatocellular carcinoma (LIHC) relates to the stemness of cancer stem cells (CSC). (A) UALCAN database analysis of SNHG3 expression in LIHC. (B) UALCAN database analysis of SNHG3 expression in LIHC with patient survival. (C) Detection of stem cell markers in CSC populations by flow cytometry. (D) EpCAM, Nanog, and SOX2 protein expression in Huh7, PLC/PRF/5, and CSC populations using Western blot. (E) SNHG3 expression in Huh7, PLC/PRF/5, and CSC populations using RT-qPCR. Data are presented as mean ± SD and analyzed using one-way/two-way ANOVA. $^{**}p < 0.01$.

in Huh7/CSC and PLC/PRF/5/CSC cell lines (Figure 1D), along with elevated expression of SNHG3 (Figure 1E).

3.2 | Depletion of SNHG3 hinders self-renewal properties of CSC and curbs tumor growth

SNHG3 expression was reduced in Huh7/CSC and PLC/PRF/5/CSC using the three shRNAs. The shRNA with the highest efficiency was selected using RT-qPCR and FISH for subsequent assays (Figure 2A,B). Knockdown of SNHG3 decreased the expression of stemness-associated genes in Huh7/CSC and PLC/PRF/5/CSC (Figure 2C). Depletion of SNHG3 repressed cell viability and colony formation, but its overexpression overturned this effect in osteosarcoma.[23] Furthermore, knockdown of SNHG3 restrained the tumor growth of prostate cancer cells and elevated methionine dependence in vivo.[24] Soft agar colony formation and sphere-forming assays revealed a significant decrease in colony formation and sphere-forming abilities of Huh7/CSC and PLC/PRF/5/CSC cells in response to SNHG3 inhibition (Figure 2D,E). Cell migration and invasion were reduced after SNHG3 depletion (Figure 2F,G). Loss of SNHG3 inhibited subcutaneous tumor volume and tumor weight (Figure 2H), with a significant decline in KI67 expression in tumor tissues (Figure 2I). The survival rate of mice with orthotopic implantation of Huh7/CSC with sh-SNHG3 was enhanced compared with that of the control group (Figure 2J).

3.3 | SNHG3 interacts with miR-502-3p

SNHG3 was predicted in the LncATLAS database (https://lncatlas.crg.eu/) to be predominantly localized in the cytoplasm of LIHC cells (Figure 3A), which was further confirmed in Huh7/CSC and PLC/PRF/5/CSC cells using FISH (Figure 3B). We then predicted miRNAs sharing interaction sites with SNHG3 in the Starbase database, followed by the intersection with the differentially expressed miRNAs in LIHC-related GSE108724 and GSE166348 (Figure 3C). Four differentially expressed miRNAs,

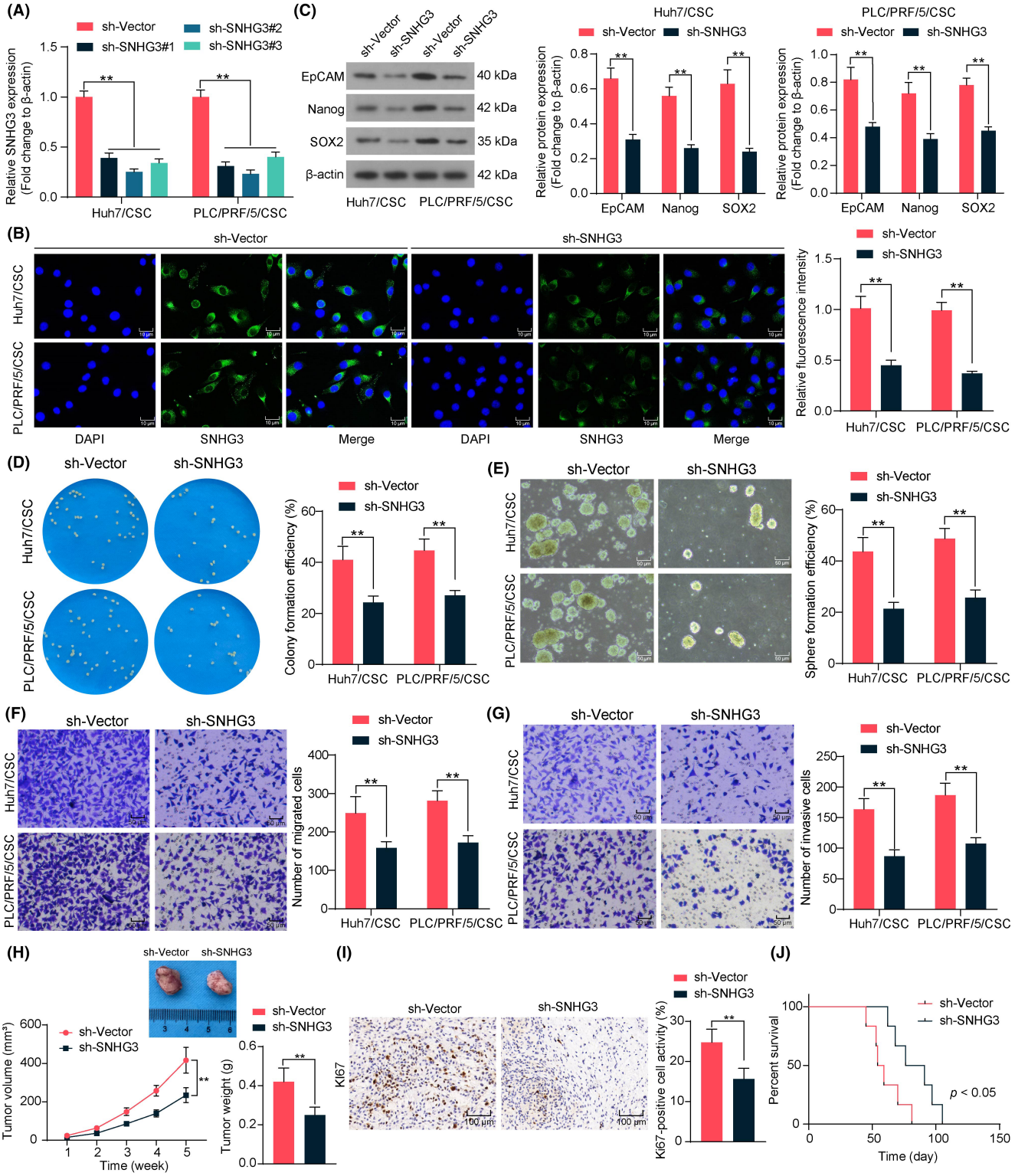

FIGURE 2 SNHG3 depletion reduces the stemness of cancer stem cells (CSC) and tumor growth in liver hepatocellular carcinoma (LIHC). SNHG3 expression after knockdown of SNHG3 in CSC populations using RT-qPCR (A) and FISH (B). (C) EpCAM, Nanog, and SOX2 protein expression in CSC populations using Western blot. The colony formation (D), sphere-forming ability (E), migration (F), and invasion (G) of CSC populations were assessed. (H) The tumor growth of mice injected with CSC populations. (I) Immunohistochemical detection of KI67 in subcutaneous tumor tissues. (J) Survival in mice with in situ liver tumors. Data are presented as mean ± SD ($n = 6$) and analyzed using unpaired *t*-test or two-way ANOVA. $^{**}p < 0.01$.

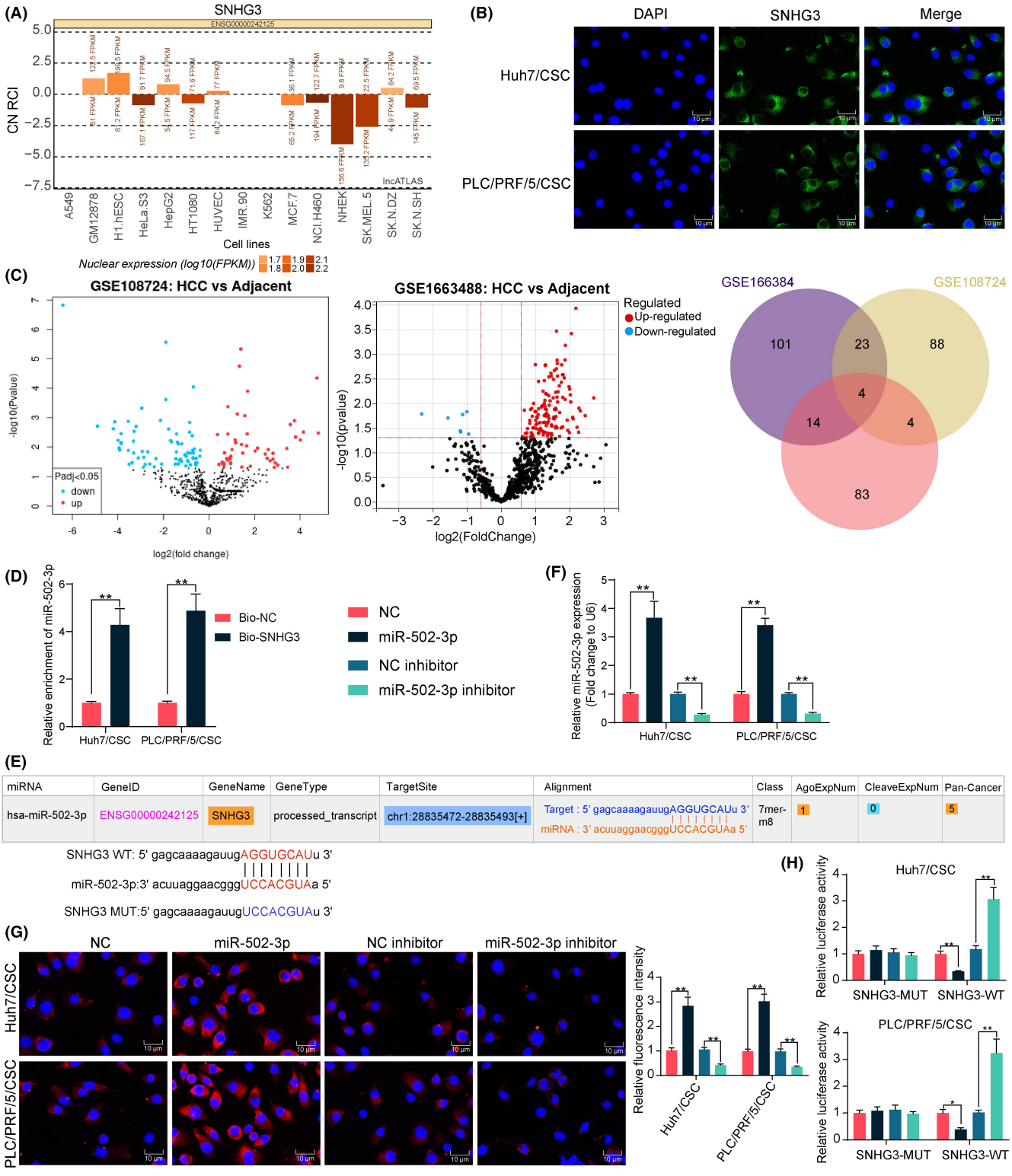

FIGURE 3 SNHG3 competitively binds to miR-502-3p. (A) The localization of SNHG3 predicted in the LncATLAS database. (B) FISH detection of SNHG3 localization in cancer stem cell (CSC) populations. (C) The intersection of differentially expressed genes and miRNA targets of SNHG3 in the Starbase database. (D) The binding relationship between SNHG3 and miR-502-3p was analyzed using RNA pull-down. (E) Analysis of SNHG3 binding sites to miR-502-3p and binding site mutation sequence design by the Starbase database. miR-502-3p expression after miR-502-3p or inhibitor treatment in CSC populations by RT-qPCR (F) and FISH (G). (H) The luciferase activity in CSC populations was analyzed using a dual-luciferase reporter assay. Data are presented as mean ± SD and analyzed using two-way ANOVA. $^{**}p<0.05$, $^{**}p<0.01$.

hsa-miR-500a-3p, hsa-miR-502-3p, hsa-miR-151a-3p, and hsa-miR-196b-5p, were screened. miR-502-3p was also identified to interact with circular RNA ribosomal protein L15 in gastric cancer[25] and lncRNA PRKAG2-AS1 in LIHC.[26] Therefore, miR-502-3p was selected as the miRNA of interest.

RT-qPCR and FISH showed that miR-502-3p expression was reduced in the collected LIHC tissues (Figure S2A,B). RNA pull-down experiments confirmed the binding relationship between SNHG3 and miR-502-3p (Figure 3D). Next, we obtained the binding sites of SNHG3 for miR-502-3p from the Starbase database and mutated the binding site (Figure 3E). Huh7/CSC and PLC/PRF/5/CSC were transfected with miR-502-3p or inhibitor, followed by efficiency validation using RT-qPCR and FISH (Figure 3F,G). The relative luciferase activity of SNHG3-WT was significantly reduced or augmented upon transfection with miR-502-3p or inhibitor, respectively (Figure 3H).

3.4 | miR-502-3p inhibitor compromises the tumor-suppressive effects of sh-SNHG3

As expected, miR-502-3p expression was lower in Huh7/CSC and PLC/PRF/5/CSC cells than in Huh7 and PLC/PRF/5 cells (Figure 4A,B). miR-502-3p inhibitor was used to infect Huh7/CSC and PLC/PRF/5/CSC with SNHG3 knockdown, and miR-502-3p was downregulated after infection in the cells (Figure 4C,D). Intervention with miR-502-3p inhibitor increased the expression of EpCAM, Nanog, and SOX2 in cells (Figure 4E), and a significant promotion in the colony formation and sphere-forming ability of Huh7/CSC and PLC/PRF/5/CSC (Figure 4F,G) and a significant elevation in the migration and invasion of cells were observed (Figure 4H,I). Inhibition of miR-502-3p accelerated subcutaneous tumor growth, as evidenced by an increase in tumor volume and weight (Figure 4J) and an increase in the number of Ki67-positive cells in the tumor tissue (Figure 4K). miR-502-3p inhibitor caused shorter surviving days in mice (Figure 4L).

3.5 | miR-502-3p targets YTHDF3 to suppress ITGA6 expression

m6A is a ubiquitous post-transcriptional modification of RNA, and abnormal m6A modification is tightly linked to LIHC progression.[27,28] The m6A-related regulators, including writers (METTL3, METTL14, METTL5, and METTL16), erasers (ALKBH5, ALKBH3, and FTO), and readers (YTHDF1, YTHDF2, YTHDF3, YTHDC1, and YTHDC2) cooperatively maintain the dynamic and reversible balance of m6A methylation.[29] As YTHDF3 has been a research target and ITGA6 is a target of YTHDF3 in our previous study regarding LIHC,[13] we wondered whether miR-502-3p targeted YTHDF3 to mediate the expression of ITGA6 in LIHC. In the StarBase database, miR-502-3p was found to bind to YTHDF3 (Figure 5A), so we speculated that miR-502-3p regulates ITGA6 expression through YTHDF3. YTHDF3 expression was elevated in LIHC according to the Starbase database (Figure 5B).

YTHDF3 expression was elevated in clinical LIHC tissues, and miR-502-3p was negatively correlated with YTHDF3 expression (Figure S2C). Western blot analysis also revealed significantly elevated YTHDF3 expression in LIHC tissues (Figure S2D). YTHDF3 mRNA and protein expression was detected in Huh7/CSC and PLC/PRF/5/CSC infected with sh-SNHG3 alone or in combination with miR-502-3p inhibitor. SNHG3 inhibition led to a decrease in YTHDF3 expression, and the miR-502-3p inhibitor partially restored YTHDF3 expression in the presence of sh-SNHG3 (Figure 5C,D). The binding relationship between miR-502-3p and YTHDF3 was confirmed using an RNA pull-down assay (Figure 5E). We mutated the binding sites of miR-502-3p and YTHDF3 and observed that the luciferase activity of YTHDF3-WT was decreased upon transfection with miR-502-3p and increased following transfection with miR-502-3p inhibitor (Figure 5F).

StarBase analysis showed elevated ITGA6 expression in LIHC (Figure 5G). Consistently, our enrolled patients with LIHC showed an upregulation of ITGA6, which was positively correlated with YTHDF3 expression (Figure S2E). RIP experiments confirmed the binding of YTHDF3 to the ITGA6 mRNA (Figure 5H). Huh7/CSC and PLC/PRF/5/CSC cells with a YTHDF3 knockdown were generated. After verifying transfection efficiency, we observed that YTHDF3 downregulation contributed to a decline in the protein expression of YTHDF3 and ITGA6 (Figure 5I,J). SNHG3 inhibition led to a remarkable decline in the protein expression of ITGA6, whereas the miR-502-3p inhibitor significantly augmented IGTA6 protein expression in the cells (Figure 5K).

3.6 | YTHDF3 promotes the translation of ITGA6 in LIHC

We overexpressed ITGA6 in Huh7/CSC and PLC/PRF/5/CSC based on the knockdown of YTHDF3 or knockdown of SNHG3, in which ITGA6 expression was significantly restored (Figure 6A). Knockdown of YTHDF3 decreased stemness-related gene expression, whereas overexpression of ITGA6 contributed to the upregulation of tumor stemness-related genes (Figure 6B). The colony-forming ability and sphere-forming ability of Huh7/CSC and PLC/PRF/5/CSC were reduced following knockdown of YTHDF3, and the self-renewal ability of Huh7/CSC and PLC/PRF/5/CSC was enhanced after overexpression of ITGA6 in addition to YTHDF3 or SNHG3 knockdown (Figure 6C,D). Transwell assays confirmed the repressive effect of YTHDF3 and SNHG3 knockdown on cell migration and invasion was reversed by ITGA6 (Figure 6E,F). Depletion of YTHDF3 inhibited subcutaneous tumor growth, whereas overexpression of ITGA6 promoted tumor growth (Figure 6G), which occurred concomitantly with the elevated KI67 expression (Figure 6H). Knockdown of YTHDF3 prolonged the survival of tumor-bearing mice, whereas ITGA6 diminished the effect of the knockdown of SNHG3 and YTHDF3 and shortened the survival of mice (Figure 6I).

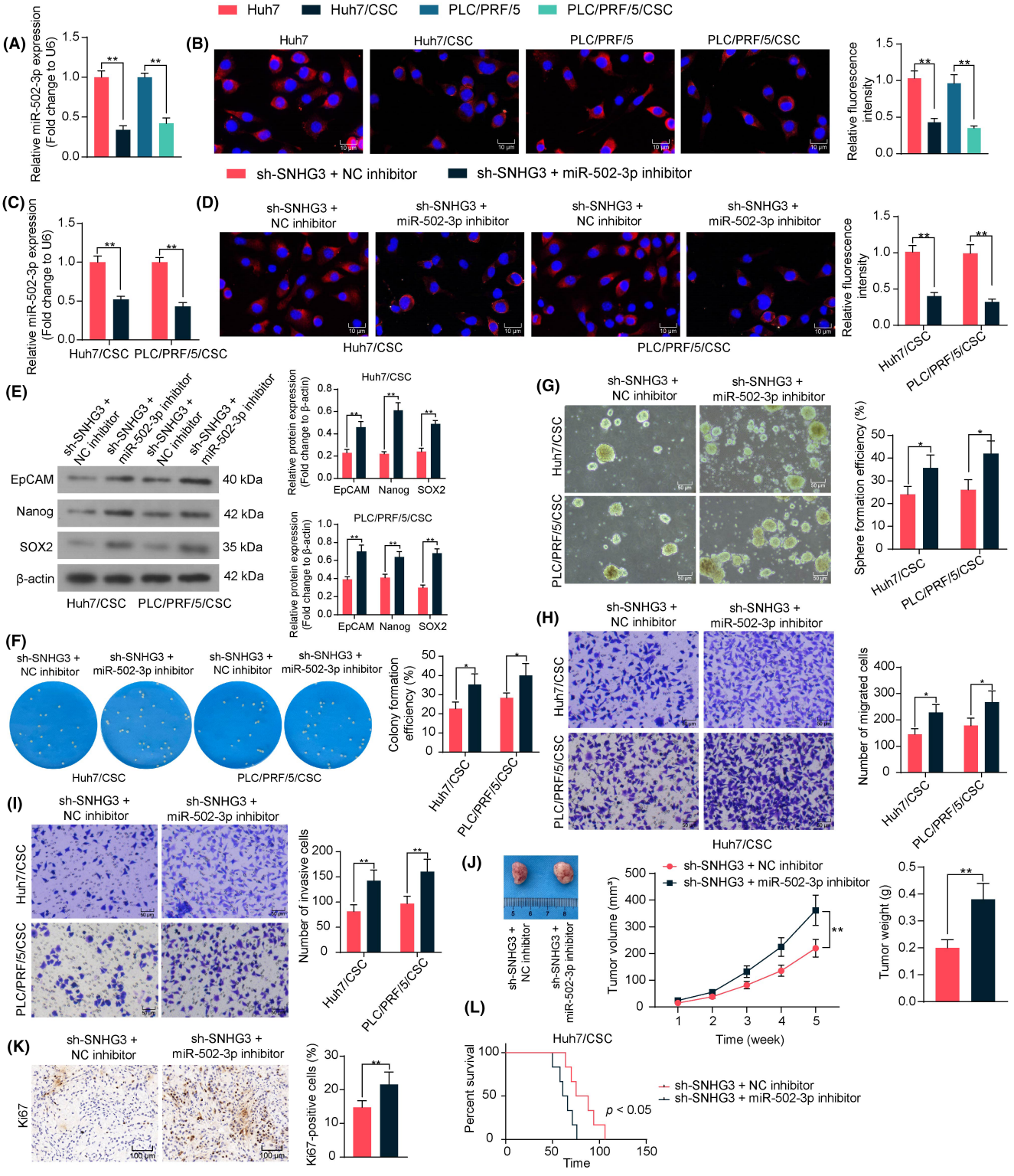

FIGURE 4 miR-502-3p inhibitor counteracts the inhibitory effect of sh-SNHG3 on stemness of liver hepatocellular carcinoma (LIHC) cells. miR-502-3p expression in Huh7, PLC/PRF/5, and cancer stem cell (CSC) population by RT-qPCR (A) and FISH (B). miR-502-3p expression in CSC populations after infection with sh-SNHG3 + miR-502-3p inhibitor by RT-qPCR (C) and FISH (D). (E) EpCAM, Nanog, and SOX2 protein expression in CSC populations using Western blot. The colony formation (F), sphere-forming ability (G), migration (H), and invasion (I) of CSC populations were assessed. (J) The tumor growth of mice injected with CSC populations. (K) Immunohistochemical detection of KI67 expression in subcutaneous tumor tissues. (L) Survival in mice with in situ liver tumors. Data are presented as mean ± SD ($n = 6$) and compared using unpaired *t*-test or one-way or two-way ANOVA. $^{*}p < 0.05$, $^{**}p < 0.01$.

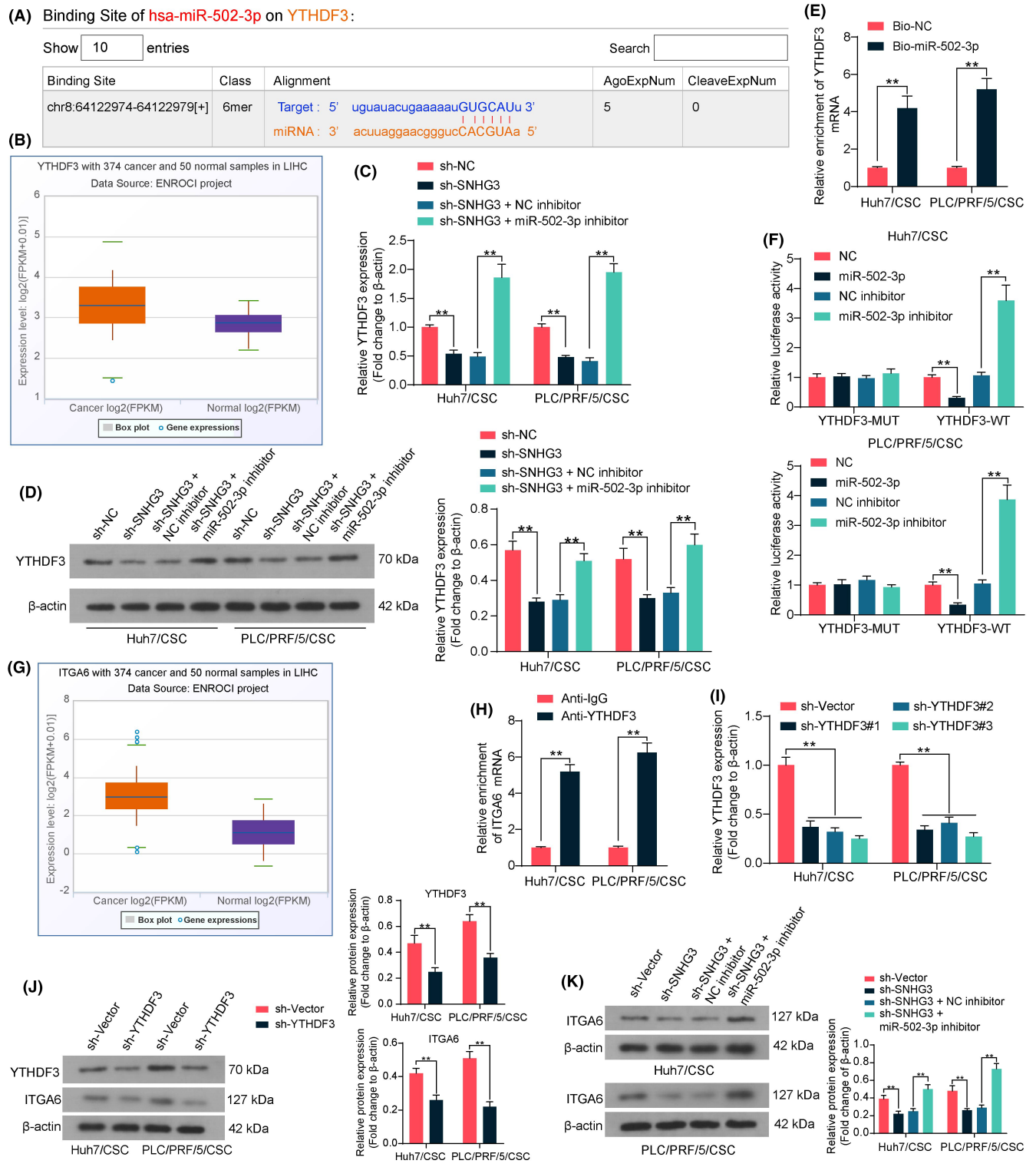

FIGURE 5 Inhibition of YTHDF3 by miR-502-3p suppresses ITGA6 expression. The binding sites between miR-502-3p and YTHDF3 (A) and YTHDF3 expression in liver hepatocellular carcinoma (LIHC) (B) were predicted using the Starbase database. YTHDF3 expression in cancer stem cell (CSC) populations with sh-SNHG3 or with miR-502-3p inhibitor by RT-qPCR (C) and Western blot analysis (D). The binding relationship between miR-502-3p and YTHDF3 in CSC populations was analyzed using RNA pull-down assay (E) and dual-luciferase reporter assays (F). (G) Starbase database analysis of ITGA6 expression in LIHC. (H) The binding relationship between YTHDF3 and ITGA6 in CSC populations using RIP assay. (I) YTHDF3 mRNA expression in CSC populations after sh-YTHDF3. YTHDF3 and ITGA6 protein expression in CSC populations after sh-YTHDF3 (J) or ITGA6 protein expression in CSC populations after sh-SNHG3 alone or with miR-502-3p inhibitor (K). Data are presented as mean ± SD and compared using paired two-way ANOVA and Tukey's post hoc test. $^{**}p < 0.01$.

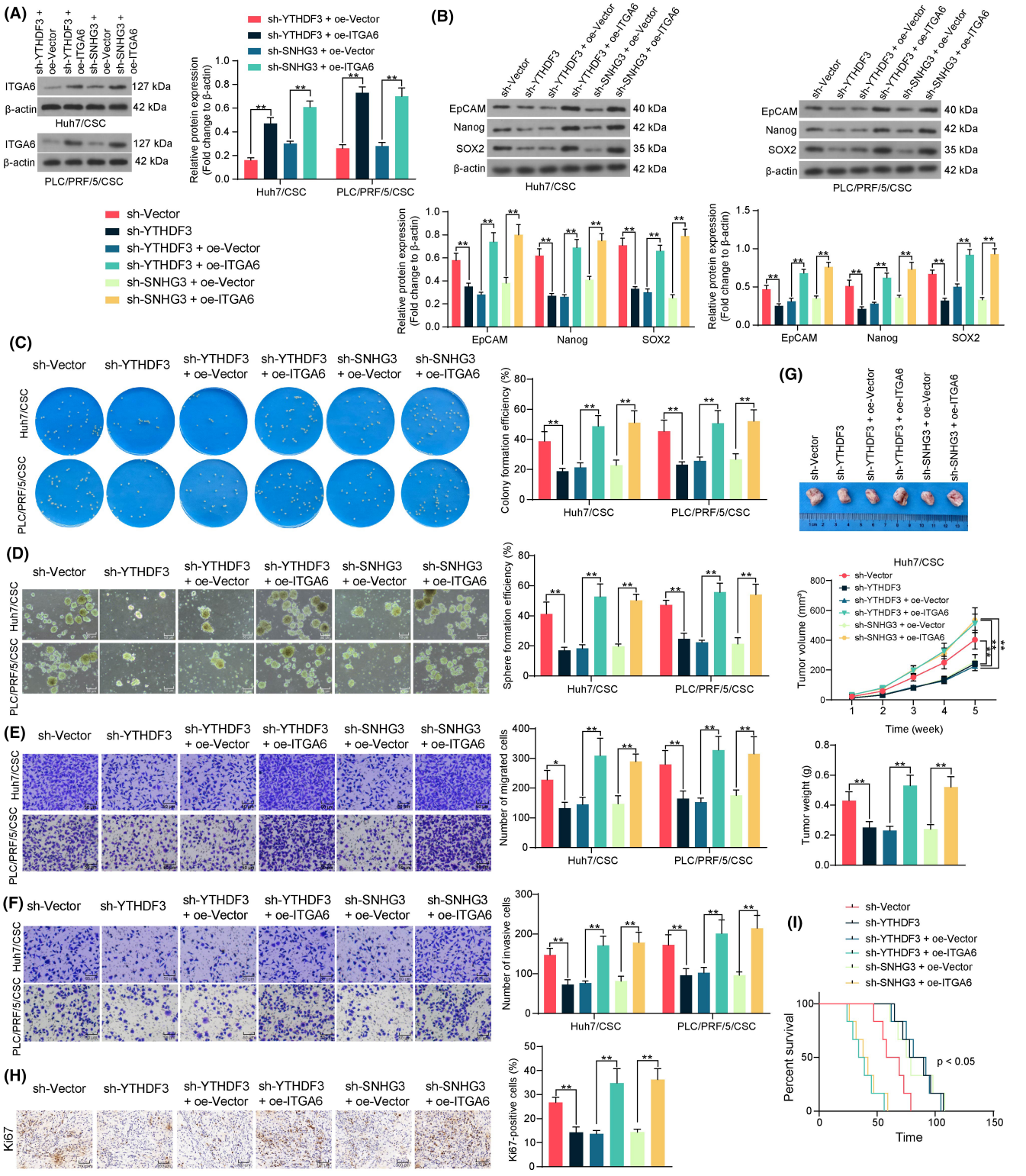

FIGURE 6 YTHDF3 promotes the translation of ITGA6 in liver hepatocellular carcinoma (LIHC). (A) ITGA6 protein expression in cancer stem cell (CSC) populations after ITGA6 overexpression in the presence of sh-YTHDF3 or sh-SNHG3 using Western blot. (B) EpCAM, Nanog, and SOX2 protein expression in CSC populations using Western blot. The colony formation (C), sphere-forming ability (D), migration (E), and invasion (F) of CSC populations were assessed. (G) The tumor growth of mice injected with CSC populations. (H) Immunohistochemical detection of KI67 expression in subcutaneous tumor tissues. (I) Survival in mice with in situ liver tumors. Data are presented as mean ± SD ($n = 6$) and compared using one-way or two-way ANOVA. $^{*}p < 0.05$, $^{**}p < 0.01$.

3.7 | METTL3-mediated m6A modification expedites ITGA6 translation

METTL3 has been documented as an essential methyltransferase and indispensable for the performance of m6A modification. METTL3 controls RNA expression in an m6A-dependent manner, thereby involving carcinogenesis, tumor progression, and drug resistance in LIHC.[30] Moreover, ITGA6 was associated with the promotion of METTL3 expression in human bladder cancer tissues, and ITGA6 upregulation in patients indicated lower survival.[31] Therefore, we postulated that the METTL3-catalyzed ITGA6 m6A modification was also responsible for the oncogenic role of ITGA6 in LIHC. Surprisingly, we found that m6A methylation of ITGA6 was significantly higher in Huh7/CSC and PLC/PRF/5/CSC than in Huh7 and PLC/PRF/5 cells, respectively (Figure 7A). The StarBase database demonstrated that METTL3 was overexpressed in LIHC (Figure 7B).

In our cohort, METTL3 was highly expressed in LIHC tissues compared with adjacent tissues, and its expression was positively correlated with ITGA6 expression (Figure S3A–B). Overexpression of METTL3 at both the mRNA and protein levels was detected in Huh7/CSC and PLC/PRF/5/CSC but not in Huh7 and PLC/PRF/5 cells (Figure 7C,D). We overexpressed METTL3 in Huh7/CSC and PLC/PRF/5/CSC cells, and RT-qPCR and Western blot analysis verified successful transfection (Figure 7E,F). The global m6A methylation (Figure 7G) and the m6A methylation level of ITGA6 mRNA (Figure 7H) in Huh7/CSC and PLC/PRF/5/CSC cells were remarkably enhanced after ectopic expression of METTL3. RIP experiments confirmed the binding of METTL3 to the ITGA6 mRNA (Figure 7I). Huh7/CSC- and PLC/PRF/5/CSC-overexpressing METTL3 were subjected to YTHDF3 knockdown, and RT-qPCR was conducted to verify the transfection efficiency (Figure 7J). ITGA6 protein expression was elevated after ectopic expression of METTL3, while it was partially decreased after YTHDF3 knockdown (Figure 7K).

3.8 | miR-502-3p targets HBXIP to repress METTL3-mediated ITGA6 expression

Interestingly, HBXIP promoted gastric cancer via m6A modification of MYC mRNA governed by METTL3.[32] There was a predicted binding site between miR-502-3p and HBXIP (LAMTOR5) in the Starbase database, and HBXIP was highly expressed in LIHC (Figure 8A). We speculated that miR-502-3p, which inhibited ITGA6 expression by targeting YTHDF3 in LIHC, can also affect METTL3 expression by targeting HBXIP and eventually repress ITGA6.

HBXIP mRNA and protein expression were also significantly elevated in LIHC tissues of our cohort (Figure S3C). Moreover, HBXIP mRNA expression shared a negative correlation with miR-502-3p expression and a positive correlation with METTL3 and ITGA6 expression (Figure S3D). HBXIP mRNA and protein expression was higher in Huh7/CSC and PLC/PRF/5/CSC than in Huh7 and PLC/PRF/5 cells, respectively (Figure 8B,C). In Huh7/CSC and PLC/PRF/5/CSC, depletion of SNHG3 suppressed the expression of HBXIP and METTL3, while miR-502-3p inhibitor upregulated HBXIP and METTL3 (Figure 8D,E). RNA pull-down assays confirmed the binding relationship between miR-502-3p and HBXIP (Figure 8F). Similarly, we mutated the binding sites of miR-502-3p and HBXIP and found that the luciferase activity of Huh7/CSC and PLC/PRF/5/CSC with the mutated binding site was insignificantly affected by miR-502-3p or miR-502-3p inhibitor (Figure 8G).

Next, we performed a knockdown of HBXIP in Huh7/CSC and PLC/PRF/5/CSC, followed by RT-qPCR to verify the knockdown efficiency (Figure 8H). METTL3 expression showed a significant reduction upon sh-HBXIP infection (Figure 8I). As a consequence, the protein expression of HBXIP, METTL3, and ITGA6 was downregulated as well (Figure 8J). Further overexpression of METTL3 was performed on Huh7/CSC and PLC/PRF/5/CSC with HBXIP knockdown, and RT-qPCR showed a significant promotion in METTL3 expression (Figure 8K). A significant increase in ITGA6 protein expression after METTL3 overexpression intervention was observed (Figure 8L). The m6A methylation on ITGA6 mRNA was decreased following HBXIP silencing, which was reversed by METTL3 (Figure 8M). The m6A methylation of ITGA6 was assessed in Huh7/CSC and PLC/PRF/5/CSC with sh-SNHG3 alone or in combination with miR-502-3p inhibitor. SNHG3 knockdown decreased the m6A modification on ITGA6, and miR-502- 3p inhibitor increased the m6A modification (Figure 8N).

3.9 | The HBXIP/METTL3/ITGA6 axis is involved in influencing stemness in LIHC

Western blot showed that suppression of HBXIP resulted in an upregulation in the expression of EpCAM, Nanog, and SOX2, which was reversed by overexpression of METTL3 (Figure S4A). Similarly, the knockdown of HBXIP significantly decreased the colony formation and sphere-forming ability of CSC, and then METTL3 overexpression strengthened the number of colony formation and sphere-forming significantly (Figure S4B,C). Overexpression of METTL3 resulted in increased migratory and invasive activity of CSC in the presence of HBXIP loss (Figure S4D,E).

We demonstrated that (1) SNHG3 was an oncogenic lncRNA and may be a biomarker of LIHC and (2) SNHG3 had effects on LIHC progression by promoting CSC self-renewal through the miR-502-3p-mediated YTHDF3/ITGA6 and HBXIP/METTL3/ITGA6 pathways (Figure 9). The above findings suggest that SNHG3 may become a promising target for LIHC and provide a strategy for LIHC treatment.

AUTHOR CONTRIBUTIONS

Juncheng Guo: Conceptualization; formal analysis; funding acquisition; methodology; writing – original draft; writing – review and editing. **Jianquan Zhang:** Data curation; investigation; visualization; writing – original draft. **Yang Xiang:** Data curation; formal analysis; investigation. **Shuai Zhou:** Methodology; software; visualization; writing – review

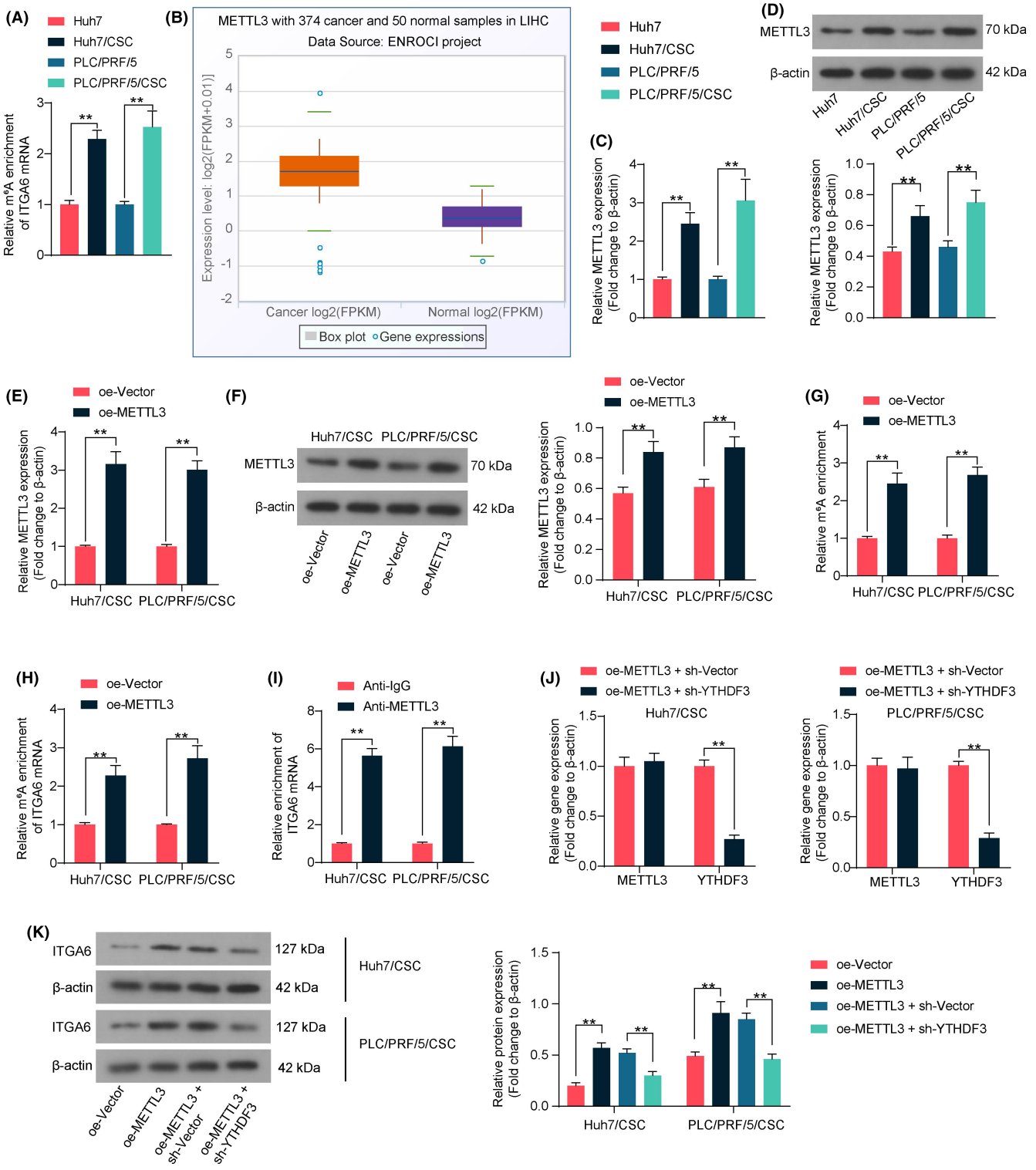

FIGURE 7 METTL3-mediated m6A modification promotes ITGA6 translation via YTHDF3. (A) The m6A methylation of ITGA6 in Huh7, PLC/PRF/5, and cancer stem cell (CSC) populations by m6A-IP-qPCR. (B) Starbase database analysis of METTL3 expression in liver hepatocellular carcinoma (LIHC). METTL3 expression in Huh7, PLC/PRF/5, and CSC populations by RT-qPCR (C) and Western blot analysis (D) and CSC populations overexpressing METTL3 by RT-qPCR (E) and Western blot analysis (F). Global m6A methylation (G) and m6A methylation of ITAG6 (H) in CSC populations overexpressing METTL3. (I) The binding relationship between METTL3 and ITGA6 mRNA was analyzed using RIP assays. METTL3 and YTHDF3 mRNA expression (J) and ITGA6 protein expression (K) in CSC populations after knockdown of YTHDF3 based on METTL3 overexpression. Data are presented as mean ± SD and compared using one-way/two-way ANOVA. $^{**}p < 0.01$.

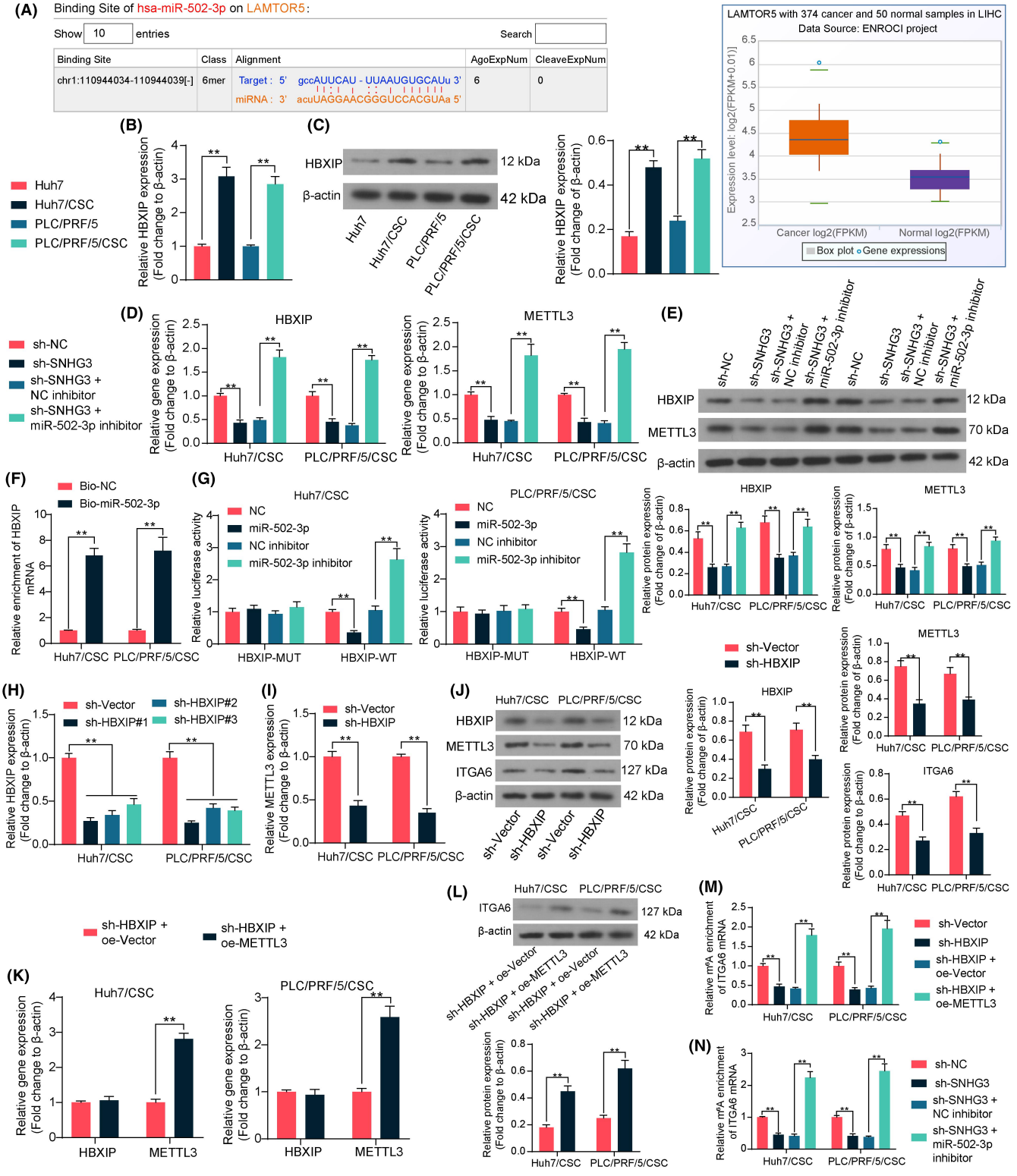

FIGURE 8 miR-502-3p targets HBXIP to regulate METTL3-mediated ITGA6 expression. (A) Starbase database prediction of binding sites between miR-502-3p and HBXIP and analysis of HBXIP expression in liver hepatocellular carcinoma (LIHC). HBXIP mRNA (A) and Protein (B) expression in Huh7, PLC/PRF/5, and cancer stem cell (CSC) populations (C). HBXIP and METTL3 mRNA (D) and Protein (E) expression in CSC populations with sh-SNHG3 alone or with miR-502-3p inhibitor using RT-qPCR and western blots analysis. The binding relationship between miR-502-3p and HBXIP using RNA pull-down assays (F) and dual-luciferase reporter assay (G). HBXIP (H) and METTL3 (I) expression in CSC populations with sh-HBXIP using RT-qPCR. (J) HBXIP, METTL3, and ITGA6 protein expression in CSC populations with sh-HBXIP using Western blot. (K) HBXIP and METTL3 expression in CSC populations with sh-HBXIP + oe-METTL3 using RT-qPCR. (L) ITGA6 protein expression in CSC populations with sh-HBXIP + oe-METTL3 using Western blot. The m6A levels of ITGA6 in CSC populations with sh-HBXIP alone or with oe-METTL3 (M) and in CSC populations with sh-SNHG3 or with miR-502-3p inhibitor (N) by m6A-IP-qPCR. Data are presented as mean ± SD and compared using one-way/two-way ANOVA. $^{*}p < 0.05$, $^{**}p < 0.01$.

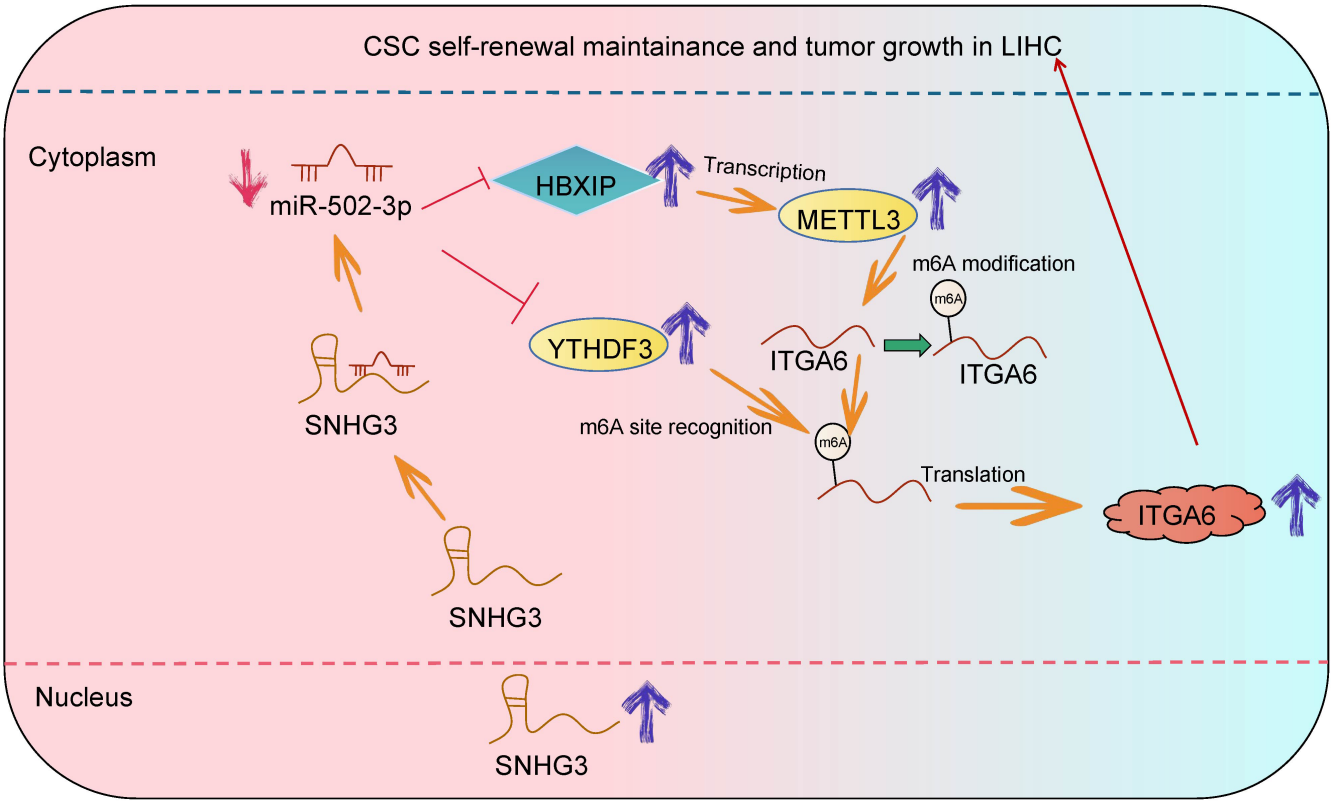

FIGURE 9 SNHG3 interacts with miR-502-3p to regulate YTHDF3 or HBXIP, thus manipulating ITGA6 translation and the m6A modification of ITGA6 by METTL3 in LIHC.

and editing. **Yijun Yang:** Funding acquisition; resources; visualization; writing – review and editing. **Jinfang Zheng:** Conceptualization; data curation; validation; writing – review and editing.

ACKNOWLEDGEMENTS

We thank to the Science and Technology Project of Hainan Province (No. ZDYF2022SHFZ117) for the funding support.

FUNDING INFORMATION

This work was supported by the Science and Technology Project of Hainan Province (No. ZDYF2022SHFZ117).

CONFLICT OF INTEREST STATEMENT

The authors have no conflict of interest.

ETHICS STATEMENTS

Approval of the research protocol by an Institutional Reviewer Board: This study was approved by the Ethics Committee of Central South University Xiangya School of Medicine Affiliated Haikou Hospital. All procedures were conducted in adherence with the Declaration of Helsinki.

Informed Consent: N/A.

Registry and the Registration No. of the study/trial: N/A.

Animal Studies: All animal procedures were approved by the Animal Ethics Committee of Central South University Xiangya School of Medicine Affiliated Haikou Hospital.

ORCID

Jinfang Zheng https://orcid.org/0000-0002-0244-8461

REFERENCES

1. Villanueva A. Hepatocellular carcinoma. *N Engl J Med*. 2019;380(15):1450-1462.
2. Kim E, Viatour P. Hepatocellular carcinoma: old friends and new tricks. *Exp Mol Med*. 2020;52(12):1898-1907.
3. Yang JD, Hainaut P, Gores GJ, Amadou A, Plymoth A, Roberts LR. A global view of hepatocellular carcinoma: trends, risk, prevention and management. *Nat Rev Gastroenterol Hepatol*. 2019;16(10):589-604.
4. Liu YC, Yeh CT, Lin KH. Cancer stem cell functions in hepatocellular carcinoma and comprehensive therapeutic strategies. *Cells*. 2020;9(6):1331.
5. Huang Z, Zhou JK, Peng Y, He W, Huang C. The role of long noncoding RNAs in hepatocellular carcinoma. *Mol Cancer*. 2020;19(1):77.
6. Han TS, Hur K, Cho HS, Ban HS. Epigenetic associations between lncRNA/circRNA and miRNA in hepatocellular carcinoma. *Cancers (Basel)*. 2020;12(9):2622.
7. Yang H, Jiang Z, Wang S, et al. Long non-coding small nucleolar RNA host genes in digestive cancers. *Cancer Med*. 2019;8(18):7693-7704.
8. Xu B, Mei J, Ji W, et al. LncRNA SNHG3, a potential oncogene in human cancers. *Cancer Cell Int*. 2020;20(1):536.
9. Zhang Q, Cheng M, Fan Z, Jin Q, Cao P, Zhou G. Identification of cancer cell Stemness-associated Long noncoding RNAs for predicting prognosis of patients with hepatocellular carcinoma. *DNA Cell Biol*. 2021;40(8):1087-1100.
10. Jiang C, Long J, Liu B, et al. miR-500a-3p promotes cancer stem cells properties via STAT3 pathway in human hepatocellular carcinoma. *J Exp Clin Cancer Res*. 2017;36(1):99.

11. Li B, Xia Y, Lv J, et al. miR-151a-3p-rich small extracellular vesicles derived from gastric cancer accelerate liver metastasis via initiating a hepatic stemness-enhancing niche. *Oncogene*. 2021;40(43):6180-6194.
12. Ren D, Lin B, Zhang X, et al. Maintenance of cancer stemness by miR-196b-5p contributes to chemoresistance of colorectal cancer cells via activating STAT3 signaling pathway. *Oncotarget*. 2017;8(30):49807-49823.
13. Guo JC, Liu Z, Yang YJ, Guo M, Zhang JQ, Zheng JF. KDM5B promotes self-renewal of hepatocellular carcinoma cells through the microRNA-448-mediated YTHDF3/ITGA6 axis. *J Cell Mol Med*. 2021;25(13):5949-5962.
14. Bigoni-Ordonez GD, Czarnowski D, Parsons T, Madlambayan GJ, Villa-Diaz LG. Integrin alpha6 (CD49f), the microenvironment and cancer stem cells. *Curr Stem Cell Res Ther*. 2019;14(5):428-436.
15. Yang N, Wang T, Li Q, et al. HBXIP drives metabolic reprogramming in hepatocellular carcinoma cells via METTL3-mediated m6A modification of HIF-1alpha. *J Cell Physiol*. 2021;236(5):3863-3880.
16. Li B, Jiang J, Assaraf YG, Xiao H, Chen ZS, Huang C. Surmounting cancer drug resistance: new insights from the perspective of N(6)-methyladenosine RNA modification. *Drug Resist Updat*. 2020;53:100720.
17. Dai G, Huang C, Yang J, et al. LncRNA SNHG3 promotes bladder cancer proliferation and metastasis through miR-515-5p/GINS2 axis. *J Cell Mol Med*. 2020;24(16):9231-9243.
18. Zhao L, Song X, Guo Y, Ding N, Wang T, Huang L. Long noncoding RNA SNHG3 promotes the development of non-small cell lung cancer via the miR-1343-3p/NFIX pathway. *Int J Mol Med*. 2021;48(2):147.
19. Lu N, Yin Y, Yao Y, Zhang P. SNHG3/miR-2682-5p/HOXB8 promotes cell proliferation and migration in oral squamous cell carcinoma. *Oral Dis*. 2021;27(5):1161-1170.
20. Xie Y, Rong L, He M, et al. LncRNA SNHG3 promotes gastric cancer cell proliferation and metastasis by regulating the miR-139-5p/MYB axis. *Aging (Albany NY)*. 2021;13(23):25138-25152.
21. Zhang PF, Wang F, Wu J, et al. LncRNA SNHG3 induces EMT and sorafenib resistance by modulating the miR-128/CD151 pathway in hepatocellular carcinoma. *J Cell Physiol*. 2019;234(3):2788-2794.
22. Tsui YM, Chan LK, Ng IO. Cancer stemness in hepatocellular carcinoma: mechanisms and translational potential. *Br J Cancer*. 2020;122(10):1428-1440.
23. Chen J, Wu Z, Zhang Y. LncRNA SNHG3 promotes cell growth by sponging miR-196a-5p and indicates the poor survival in osteosarcoma. *Int J Immunopathol Pharmacol*. 2019;33:2058738418820743.
24. Wang X, Song Y, Shi Y, Yang D, Li J, Yin B. SNHG3 could promote prostate cancer progression through reducing methionine dependence of PCa cells. *Cell Mol Biol Lett*. 2022;27(1):13.
25. Li Y, Gong Y, Ma J, Gong X. Overexpressed circ-RPL15 predicts poor survival and promotes the progression of gastric cancer via regulating miR-502-3p/OLFM4/STAT3 pathway. *Biomed Pharmacother*. 2020;127:110219.
26. Ou Y, Deng Y, Wang H, Zhang Q, Luo H, Hu P. Targeting antisense lncRNA PRKAG2-AS1, as a therapeutic target, suppresses malignant behaviors of hepatocellular carcinoma cells. *Front Med (Lausanne)*. 2021;8:649279.
27. Feng Q, Wang D, Xue T, et al. The role of RNA modification in hepatocellular carcinoma. *Front Pharmacol*. 2022;13:984453.
28. Sivasudhan E, Blake N, Lu ZL, Meng J, Rong R. Dynamics of m6A RNA Methylome on the hallmarks of hepatocellular carcinoma. *Front Cell Dev Biol*. 2021;9:642443.
29. Qu N, Bo X, Li B, et al. Role of N6-Methyladenosine (m(6)a) methylation regulators in hepatocellular carcinoma. *Front Oncol*. 2021;11:755206.
30. Pan F, Lin XR, Hao LP, Chu XY, Wan HJ, Wang R. The role of RNA Methyltransferase METTL3 in hepatocellular carcinoma: Results and perspectives. *Front Cell Dev Biol*. 2021;9:674919.
31. Jin H, Ying X, Que B, et al. N(6)-methyladenosine modification of ITGA6 mRNA promotes the development and progression of bladder cancer. *EBioMedicine*. 2019;47:195-207.
32. Yang Z, Jiang X, Li D, Jiang X. HBXIP promotes gastric cancer via METTL3-mediated MYC mRNA m6A modification. *Aging (Albany NY)*. 2020;12(24):24967-24982.

SUPPORTING INFORMATION

Additional supporting information can be found online in the Supporting Information section at the end of this article.

How to cite this article: Guo J, Zhang J, Xiang Y, Zhou S, Yang Y, Zheng J. Long noncoding RNA SNHG3 interacts with microRNA-502-3p to mediate ITGA6 expression in liver hepatocellular carcinoma. *Cancer Sci*. 2024;115:2286-2300. doi:10.1111/cas.16190